

Analytical stress solution in hyperelastic thick-walled sphere under external pressure using different strain energy functions

Abdelhakim Benslimane^{1*}, Adel Benidir²,

¹ Laboratoire Mécanique, Matériaux et Energétique (L2ME), Département Génie Mécanique, Faculté de Technologie, Université de Bejaia, Bejaia 06000, Algérie

² Centre National d'Études et de Recherche intégrées du Bâtiment (CNERIB), Souidania-Alger 16097, Algérie

*Corresponding author abdelhakim.benslimane@univ-bejaia.dz; benslimane.ah@gmail.com

Received: 03 January 2022; Accepted: 25 January 2022; Published: 30 January 2022

Abstract

Due to their large deformation, rubber-like materials are used in many industrial applications. However, few studies are available in the literature on the classification of rubber-like materials, their mechanical properties and the behavior of this material due to their hyperelastic and nonlinear behavior. In this work, an incompressible isotropic nonlinear elastic thick-walled spherical structure subjected to external pressure is studied using analytical formulation. The study aims to analyze the behavior and the stress field of such materials which are characterized by high deformability. Five different type strain energy functions are applied to a pressurized thick-walled hollow sphere to model the material behavior. A closed-form analytical solution is obtained and the results predicted from classic strain energy models (Neo-Hookean and Mooney Rivlin) and those obtained by Isihara, Biderman and Gent-Thomas models are compared in the prescribed case. The solution obtained, for different models, was used to determine the stress field (radial and hoop stresses) across thickness of the sphere. Finally, the influence of some parameters such as the radial pre-stretched sphere on stress components was examined. Comparisons are done to investigate the accuracy and evaluating the effectiveness of some existing constitutive models in the analysis of spherical vessel under external pressure.

Keywords: Hyperelastic; Strain Energy Functions; Thick-Walled Pressure Vessel; Analytical Solution

1. Introduction

Rubber and rubber-like materials which are assumed incompressible and isotropic materials are used in many engineering applications such as in automotive as tires, engine and transmission mounts, center bearing supports and exhaust rubber parts. The particularity of these rubber-like materials is their stress-stretch curves which are S-shaped to J-shaped forms due to their high deformability.

The mathematical modeling of such material encounters considerable difficulties related to their nonlinear behavior [1]. In recent years, many scholars have developed constitutive modeling of rubber like materials [1-5]. In order to describe the elastic behavior of elastomers, numerous models can be found in the prolific literature, but only few of them can be able to reproduce the response of the material, i.e. to satisfactorily fit experimental data for different loadings [6]. Among the various models recommended for the mechanical behavior of elastomers, the hyperelastic models are generally employed for modeling the nonlinear elastic behavior of homogeneous and isotropic polymers which exhibit large deformation [7-11]. The authors in [6] proposed a comparison of twenty different phenomenological and physical hyperelastic models for rubber-like materials. The material parameters of each model were determined by fitting to experimental data of [12]. The aim of their work [6] was to systematically compare hyperelastic models in order to classify them with respect to their ability to fit experimental

data. There has been remarkable interest to know how an appropriate strain energy function can provide the foundation of an analytical solution on prediction of response of a realistic structure which undergoes three-dimensional large deformation.

The design of thin/thick-walled hollow spherical structures made of hyperelastic material and subjected to internal pressure remains a challenging task. From a general perspective, cylindrical and spherical structures used in many industrial applications under internal and/or external pressure require rigorous stress analysis for their optimal, reliable and secure operational design. The behavior of an inflating of thin-walled cylindrical/spherical membrane under internal pressure has been investigated for large deformations by many authors [13-16]. In most cases the authors investigate the stability of hollow thin spherical membranes [17-19]. It is generally admitted that membranes and thin-walled spherical structures are successfully modeled as an ideal membrane with related mathematical simplifications.

However, in the case of thick-walled spherical structures the problem of formulation should consider the three-dimensional character of the solid. Accordingly, the analysis of the complete stress field of thick-walled spheres made of rubber-like materials by applying different hyperelastic models has received less academic interest.

In their work, Anssari-Benam [20] investigated the accuracy of a generalized neo-Hookean strain energy function to model

the two characteristic instability phenomena in the inflation of rubber-like.

Recently, Taghizadeh et al. [21] analyzed elastic behavior of cylindrical and spherical shells using different strain energy functions. The authors carried out an analytical study to investigate the stability of structures under internal pressure, where a comprehensive study was done on vanishing circumstances of the snap-through instability that occurs in the inflation of internally pressurized spherical shells and cylindrical tubes.

Debotton et al. [22] focused on axisymmetric bifurcations of thick-walled hollow spheres. The authors studied the mechanical behavior of a thick-walled spherical shell during inflation using four different material models. They investigated the existence of local pressure maxima and minima and the dependence of the corresponding stretches on the material model and shell thickness.

The present work places emphasis on the analytical formulation of the distribution of stresses across the thickness of thick-walled spherical structure subjected to external pressure. The analytical solutions are proposed for different constitutive models to study the inflation of a hyperelastic material as the material parameters are identified by using experimental calibration for various strain energy functions. In Section 2, the basic equations are developed for a sphere made of hyperelastic isotropic homogeneous material. Section 3 gives the results and the analysis of the sphere are described and discussed.

II. Mathematical formulation

We consider a hollow sphere made of an incompressible isotropic hyperelastic material. The sphere has inner and outer radii, noted A and B, respectively and subjected to an external pressure (labeled P_{out}). The schematic view of the thick sphere is shown in Figure 1, where the initial and the current configurations are detailed.

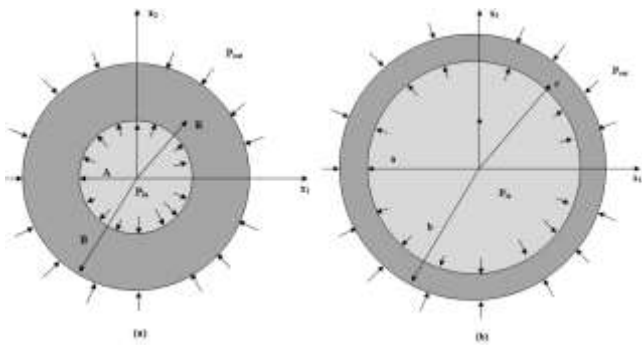


Figure 1 Thick-walled sphere with wall made of hyperelastic material, (a) initial configuration (b) current configuration.

Considering the symmetry of the geometry and the axisymmetric load conditions, it is more appropriate to consider a spherical coordinate system (r, θ, φ).

If (R, Θ, Φ) and (r, θ, φ) are coordinates of the rubber sphere before and after deformation respectively, the deformation pattern of the rubber sphere can be expressed as [5]:

$$r = f(R), \quad \theta = \Theta, \quad \phi = \Phi \tag{1}$$

Based on the theory of continuum mechanics, the deformation gradient tensor $\overline{\overline{F}}$ and left Cauchy green tensor $\overline{\overline{B}}$ are defined as [5]:

$$\overline{\overline{F}} = \overline{\overline{F}}^T = \begin{bmatrix} \lambda_r & 0 & 0 \\ 0 & \lambda_\theta & 0 \\ 0 & 0 & \lambda_\phi \end{bmatrix}, \quad \overline{\overline{B}} = \overline{\overline{F}}\overline{\overline{F}}^T \tag{2a, b}$$

Where λ_r , λ_θ and λ_ϕ are the principal stretches in the radial, circumferential and meridional direction of the thick-walled sphere. The stretches are expressed as follow [5]:

$$\lambda_r = \frac{dr}{dR}, \quad \lambda_\theta = \frac{r}{R}, \quad \lambda_\phi = \frac{r}{R} \tag{3}$$

Correspondingly, the principal invariants of the left Cauchy-Green strain tensor are [5]:

$$\begin{cases} I_1 = \text{tr} \overline{\overline{B}} \\ I_2 = \frac{1}{2} \left((\text{tr} \overline{\overline{B}})^2 - \text{tr} \overline{\overline{B}}^2 \right) \\ I_3 = \det \overline{\overline{B}} \end{cases} \tag{4a,b,c}$$

Substituting Eq. (2) into Eq. (4) results in [5]:

$$\begin{cases} I_1 = \lambda_r^2 + \lambda_\theta^2 + \lambda_\phi^2 \\ I_2 = \lambda_r^{-2} + \lambda_\theta^{-2} + \lambda_\phi^{-2} \\ I_3 = \lambda_r \lambda_\theta \lambda_\phi \end{cases} \tag{5a,b,c}$$

For convenience [21]:

$$Q = \frac{R}{r} = \lambda_\theta^{-1} \tag{6}$$

It is worth noting that the present formulation based on the notation facilitates the steps and the derivation trend of the analytical solutions. It is considered that the material of the sphere is considered to be incompressible.

The resulting deformation is then described by the following equations [21]:

$$\lambda_r = Q^2, \quad r^3 = R^3 + k \tag{7}$$

It can be easily concluded:

$$\frac{dQ}{dr} = \frac{Q^{-2} - Q}{r} \tag{8}$$

The principal Cauchy stresses are given in the form of:

$$\begin{cases} \sigma_r = \frac{Q}{2} \frac{\partial W}{\partial Q} - p \\ \sigma_\theta = \sigma_\phi = -Q \frac{\partial W}{\partial Q} - p \end{cases} \tag{9}$$

where the scalar p serves as an indeterminate Lagrange multiplier.

It can be also concluded:

$$\sigma_r - \sigma_\theta = \frac{3}{2} Q \frac{dW}{dQ} \tag{10}$$

where $W(Q) = W(Q^2, Q^{-1}, Q^{-1})$

By considering nobody forces, the equilibrium equation of the axial symmetry in the current configuration can be achieved as:

$$\frac{d\sigma_r}{dr} + 2 \left(\frac{\sigma_r - \sigma_\theta}{r} \right) = 0 \tag{11}$$

Applying the chain rule for finding derivatives, we have:

$$\frac{d\sigma_r}{dr} = \frac{d\sigma_r}{dQ} \frac{dQ}{dr} \tag{12}$$

The substitution of Eqs. (8) and (10) into equilibrium equation (11) could lead to :

$$\frac{d\sigma_r}{dQ} = - \left(\frac{3}{Q^{-3} - 1} \frac{\partial W}{\partial Q} \right) \tag{13}$$

The solution of Eq.13 can be computed easily by using any well-known computer algebra system such as Maple for different strain energy functions such as Neo-Hookean, Mooney-Rivlin, Gent-Thomas, Biderman and Isihara. These models have simple mathematical forms listed below:

- Neo-Hookean strain energy function [12]:

$$W_{NH} = C_{10} (I_1 - 3) \tag{14}$$

where $C_{10} = \mu/2$ and μ is the shear modulus.

- Mooney-Rivlin strain energy function [23]:

$$W_{MR} = C_{10} (I_1 - 3) + C_{01} (I_2 - 3) \tag{15}$$

where C_{10} and C_{01} stand for the material parameters of Mooney-Rivlin model.

- Gent-Thomas strain energy function [24]:

$$W_{GT} = C_1 (I_1 - 3) + C_2 \ln \left(\frac{I_2}{3} \right) \tag{16}$$

where C_1 and C_2 are the two material parameters

- Isihara strain energy function [25]:

$$W_I = C_{10} (I_1 - 3) + C_{20} (I_1 - 3)^2 + C_{01} (I_1 - 3) \tag{17}$$

where C_{10} , C_{20} and C_{01} stand for the material parameters of Ishira model.

- Biderman strain energy function [26]:

$$W_B = C_{10} (I_1 - 3) + C_{01} (I_2 - 3) + C_{20} (I_1 - 3)^2 + C_{30} (I_1 - 3)^3 \tag{18}$$

where C_{10} , C_{01} , C_{20} and C_{30} stand for the material parameters of Biderman model.

The material parameters of each model can be identified using experimental data as shown by [6].

For example:

Gent-Thomas Model:

$$\sigma_r = 3C_1 (Q^4 + 4Q) + C_2 \left(\ln(1 + 2Q^6) + 2\sqrt{2} \arctan(\sqrt{2}Q^3) \right) + K \tag{19}$$

where the parameter K in Eq. (19) is an unknown constant that is determined using the mechanical boundary conditions. Applying a constant uniform pressure at the outer surfaces of the thick-walled pressure vessel, the boundary conditions are expressed as:

$$\sigma_r (Q_{out} = \lambda_b^{-1}) = -p_{out} \tag{20}$$

$\lambda_a = a/A$ and $\lambda_b = b/B$ are the radial stretch at the inside and outside surfaces of the sphere, respectively and are expressed by:

$$\lambda_b^3 = (\lambda_a^3 - 1)\eta^3 + 1, \quad \frac{R}{r} = \frac{1}{\sqrt[3]{1 + (\lambda_a^3 - 1)\frac{A^3}{R^3}}} \quad (21a, b)$$

where $\eta = A/B$

Here the hoop stress is obtained from Eq. (10):

$$\sigma_\theta = \sigma_\phi = \sigma_r - \frac{3}{2}Q \frac{dW}{dQ} \quad (22)$$

Assuming that the spherical shape of the pressurized sphere remains unchanged and $\Delta P = p_{in} - p_{out}$ is denoting the pressure difference between the inner and the outer surfaces:

$$\Delta P = -\sigma_r(Q_{in} = \lambda_a^{-1}) + \sigma_r(Q_{out} = \lambda_b^{-1}) \quad (23)$$

III. Numerical application

The calibrated material parameters for Gent-Thomas (W_{GT}), Ishira (W_{IS}), Biderman (W_B), Mooney Rivlin (W_{MR}) and for the neo-Hookean (W_{NH}) strain energy density functions are reported in Table 1.

Table 1 Parameters of hyperelastic models for Treloar experimental data [12].

| Type of model | Material parameters |
|---------------|--|
| Neo-Hookean | $C_{10} = 0.2$ |
| Mooney-Rivlin | $C_{10} = 0.162$ and $C_{01} = 5.90 \cdot 10^{-3}$ |
| Gent-Thomas | $C_1 = 0.176$ and $C_2 = 5.65 \cdot 10^{-2}$ |
| Ishihara | $C_{10} = 0.171$, $C_{20} = 4.89 \cdot 10^{-3}$ and $C_{01} = -2.4 \cdot 10^{-4}$ |
| Biderman | $C_{10} = 0.208$, $C_{01} = 2.33 \cdot 10^{-2}$, C_{20} and $C_{30} = -2.4 \cdot 10^{-3}$ |

The parameters of the models described by the strain density energy functions given in Eqs (14) to (18) are listed in Table 1 [6]. The parameters are derived by fitting data from the experimental results reported in Treloar [12].

In this section, we focus on the numerical results obtained for mechanical behavior modeling of these materials using five different types of strain energy density functions. These numerical computations are carried out for internal pressure and stress field.

We consider a thick sphere with the following characteristics: $A = 0.1$ m, $B = 0.2$ m. In order to determine the unknown constants in these closed-form solutions, appropriate boundary conditions should be defined. The applied external pressure is $P_{out} = 0.5$ MPa.

IV. Results and discussions

IV.1. Validation

In order to validate the calculation methodology as well as the data consistency, the results reported in [21] are taken as a benchmark. In Figure 2, the pressure differences between the inner and the outer surfaces (ΔP) as a function of the stretch λ_a

are plotted. The concordance between the outcomes of the current study and the reference (Taghizadeh et al. [21]) are evaluated by applying Mooney Rivlin (W_{MR}) and neo-Hookean (W_{NH}) strain energy density functions and by considering $\eta = 0.35$. The results from the current analytical formulation are in excellent agreement with those reported in [21]. In fact, the maximum error does not exceed 0.1%.

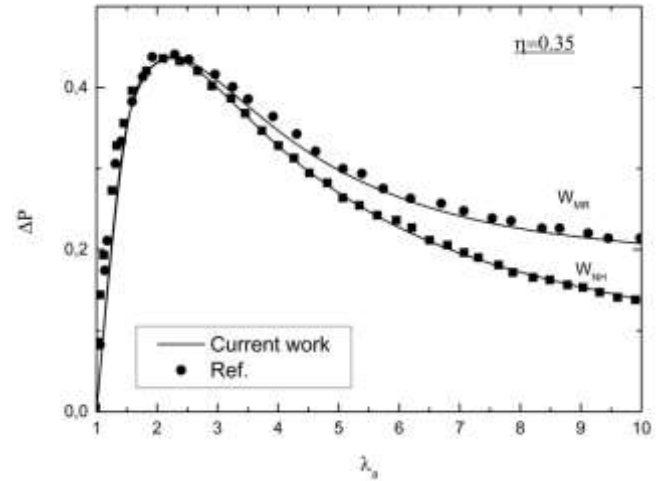


Figure 2 The pressure ΔP as a function of the stretch λ_a for the Mooney Rivlin (W_{MR}) and for the neo-Hookean (W_{NH}) strain energy density functions for $\eta = 0.35$: comparison of current results and results obtained by Ref. [21].

IV.2. Current work

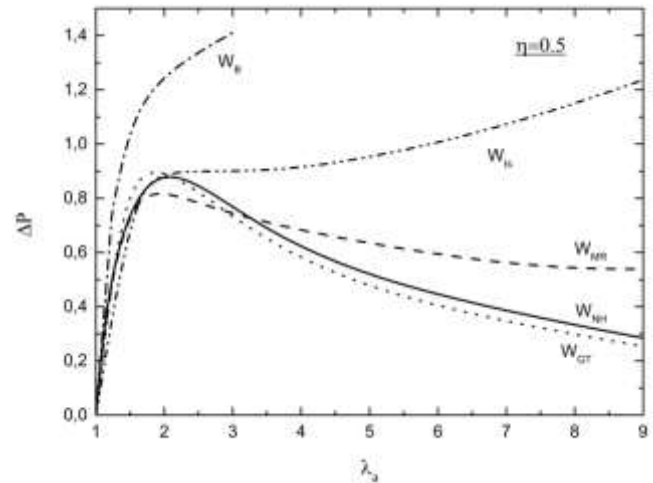


Figure 3. The pressure ΔP as a function of the stretch λ_a for the Gent-Thomas (W_{GT}), for the Ishira (W_{IS}), for the Biderman (W_B), for Mooney Rivlin (W_{MR}) and for the neo-Hookean (W_{NH}) strain energy density functions for $\eta = 0.5$.

Figure 3 illustrates the difference on the pressure ΔP as a function of the stretch λ_a for different strain energy density functions studied herein, for the case of internal to external radii ratios $\eta = 0.5$ for the spherical shell made of the rubber tested by Treloar (Treloar [12]). It could be concluded that a progressive increase of in the stretch λ_a leads to create a monotonic increase in pressure until $\lambda_a \sim 2$.

In the case of Gent-Thomas (W_{GT}), Mooney Rivlin (W_{MR}) and neo-Hookean (W_{NH}) models, the pressure curves have a single local pressure maximum and after that the pressure curves suddenly show monotonic decrease. This general observation is violated for the Ishira (W_{IS}) and the Biderman (W_B) models where the two curves remain with the same slope. Thus the evolution trend of the pressure could be classified as closer for three models whereas large dispersion is observed for the two representative curves of Ishira (W_{IS}) and the Biderman (W_B). In fact, as the stretch λ_a is higher than 2, a disproportional increase of the pressure is identified.

Figure 4a shows the radial stress distributions (σ_{rr}/P_i) in the r -direction for different strain energy functions, from which it is found that the radial stress components have its minimum values in at inner surface of the sphere ($r = A$) and its magnitude shows a monotonic behavior increasing towards the outer surface of the sphere. However, for all the applied models, the normalized radial stress is minus one at outer surface ($\sigma_{rr}/P_i(r=B) = -1$) of the sphere that satisfies the boundary conditions. The curves of the radial stresses show a divergence between models results in the outer region of the sphere.

The circumferential stress component ($\sigma_{\theta\theta}/P_i$) is a maximum at the inner surface of the hollow sphere and its magnitude shows a monotonic behavior decreasing towards the outer surface of the sphere for all the tested strain energy functions (Figure 4b). The curves of the hoop stresses remain parallel.

As shown in Figure 4, the radial stress is consistently compressive; however, the hoop stress is tensile at the inner surface and become compressive at outer surface.

V. Conclusions

In this work, the behavior of a thick-walled pressure sphere made of an incompressible isotropic nonlinearly elastic material is studied. The aim through this investigation is to examine the stress field and the response of the sphere to the imposed mechanical loading. A closed-form analytical solution was derived from the governing equations. The hyperelastic behavior was modeled by employing five different strain energy functions (Neo-Hookean, Mooney Rivlin, Gent-Thomas, Biderman and Ishihara) as established in the literature. The result analysis shows that an important divergence of the stress components is outlined as different models are applied. At the first glance, the study highlights the importance to impose a concise methodology to select models for structural designing as hyperelastic materials are in process. The difference between the results obtained based on different strain energy functions are related to the accuracy with which these models reproduce the experimental data. Mechanical loading as radial stretch is too important structural designing parameters; stress field of a thick-walled pressure sphere is examined in terms of the influence of these parameters. It was shown that the radial and hoop stress components are sensitive to the variation of radial stretch

where the higher radial stretch is applied the higher stress components are generated.

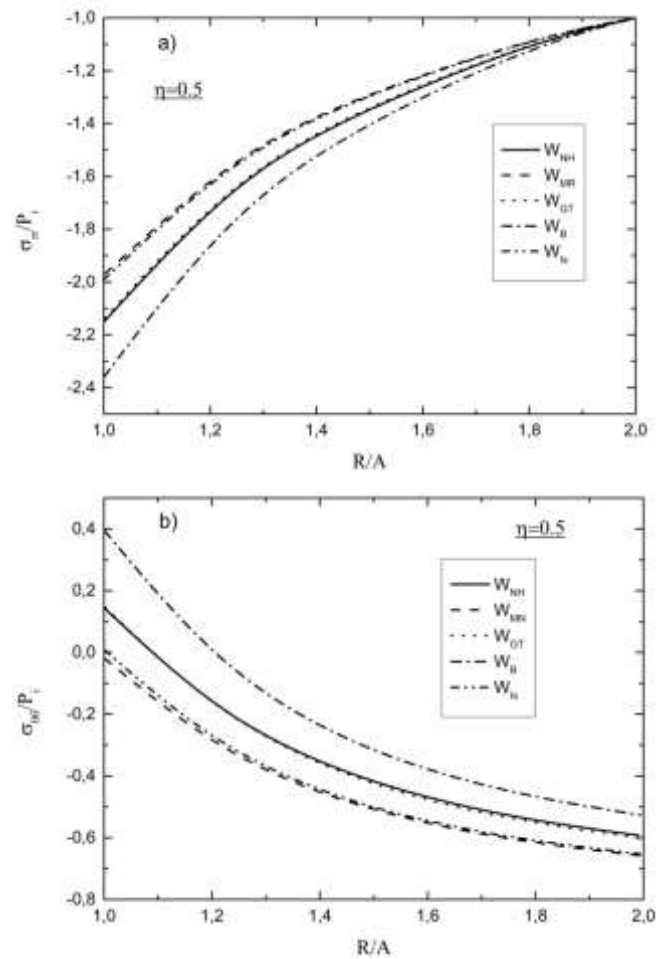


Figure 4. The normalized radial (a) and hoop (b) stresses as a function of the dimensionless radial position (R/A) of a spherical vessel made for the Gent-Thomas (W_{GT}), for the Ishira (W_{IS}), for the Biderman (W_B), for Mooney Rivlin (W_{MR}) and for the neo-Hookean (W_{NH}) strain energy density functions in the presence of radial loading $\lambda_a = 1.2$ and for $\eta = 0.5$.

Acknowledgements

The author thanks the General Directorate of Scientific Research and Technological Development (DGRSDT/MESRS-Algeria) for their financial support. We would like to thank the anonymous reviewers.

References

- [1] M.F. Beatty, Topics in Finite Elasticity: Hyperelasticity of Rubber, Elastomers, and Biological Tissues—With Examples. *App. Mech. Rev.*, 40: 5, 1699 -1735, 1987. <https://doi.org/10.1115/1.3149545>
- [2] R.S. Rivlin, Large elastic deformations of isotropic materials IV. Further developments of the general theory. *Phil. Trans. R. Soc. Lond. A* 241, 379-397, 1948. doi:10.1098/rsta.1948.0024

- [3] R.W. Ogden. Nonlinear elasticity, anisotropy, material stability and residual stresses in soft tissue (lecture notes, CISM Course on the Biomechanics of Soft Tissue in Cardiovascular Systems), 65-108, 2003. CISM Courses and Lectures Series 441, Springer, Wien
- [4] R.W. Ogden, Non-linear Elastic Deformations. Dover Publications, New York (1997)
- [5] G.A. Holzapfel, Nonlinear Solid Mechanics. A Continuum Approach for Engineering. John Wiley & Sons, Chichester (2000)
- [6] G. Marckmann, E. Verron. Comparison of hyperelastic models for rubber-like materials. Rubber Chemistry and Technology, American Chemical Society 79 (5), 835-858, 2006. <https://doi.org/10.5254/1.3547969>
- [7] A.H. Muhr. Modeling the Stress-strain Behavior of Rubber. Rubber Chemistry and Technology 78, 391-425, 2005. <https://doi.org/10.5254/1.3547890>
- [8] F. Elhaouzi, A. Nourdine, C. Brosseau, A. Mdarhri, I. El Aboudi, M. Zaghrioui. Hyperelastic Behavior and Dynamic Mechanical Relaxation in Carbon Black-Polymer Composites. Polymer Composites 40 (8), 3005-3011, 2018. <https://doi.org/10.1002/pc.25142>
- [9] H. Shin, J. Choi, M. Cho. An efficient multiscale homogenization modeling approach to describe hyperelastic behavior of polymer nanocomposites. Composite Science and Technology 175, 128-134, 2019. <https://doi.org/10.1016/j.compscitech.2019.03.015>
- [10] M.L. Ju, S. Mezghani, H. Jmal, R. Dupuis, E. Aubry. Parameter estimation of a hyperelastic constitutive model for the description of polyurethane foam in large deformation. Cellular Polymers 32(1), 21-40, 2013. <https://doi.org/10.1177/026248931303200102>
- [11] A. Karimzadeh, M.R. Ayatollahi, S.S. Rahimian Koor, A.R. Bushroa, M.Y. Yahya, & M.N. Tamin. Assessment of Compressive Mechanical Behavior of Bis-GMA Polymer Using Hyperelastic Models. Polymers 11, 1571, 2019. <https://doi.org/10.3390/polym11101571>
- [12] L.R.G. Treloar, Stress-strain data for vulcanised rubber under various types of deformation, Transactions of the Faraday Society 40 59-70, 1944. <https://doi.org/10.1039/TF9444000059>
- [13] E. Verron, R.Khayat, A. Derdouri, B. Peseux. Dynamic inflation of hyperelastic spherical membranes. Journal of Rheology. American Institute of Physics, 43, 1083-1097, 1999. <https://dx.doi.org/10.1122/1.551017>
- [14] H. Alexander, Tensile instability of initially spherical balloons. International Journal of Engineering Science 9, 151-162, 1971. [https://doi.org/10.1016/0020-7225\(71\)90017-6](https://doi.org/10.1016/0020-7225(71)90017-6)
- [15] X. C. Shang. Tensile instability of nonlinear spherical membrane with large deformation. Applied Mathematics and Mechanics 12, 993-1000, 1991. <https://doi.org/10.1007/BF02451485>
- [16] A.Goriely, M. Destrade, M. Ben Amar, Stability and bifurcation of compressed elastic cylindrical tubes. Quarterly Journal of Mechanics and Applied Mathematics 59, 615-630, 2006. <https://doi.org/10.1016/J.IJENGSCI.2006.06.014>
- [17] D.M. Haughton, Y.C. Chen, Asymptotic bifurcation results for the eversion of elastic shells, Zeitschrift für angewandte Mathematik und Physik 54 (2), 191-211, 2003. <https://doi.org/10.1007/s000330300000>
- [18] D.M. Haughton, E. Kirkinis. A Comparison of Stability and Bifurcation Criteria for Inflated Spherical Elastic Shells. Mathematics and Mechanics of Solids 8 (5), 561-572, 2003. <https://doi.org/10.1177/10812865030085008>
- [19] D. M. Haughton, Inflation and bifurcation of compressible spherical membranes, Journal of Elasticity 12, 239-245, 1982. <https://doi.org/10.1007/BF00042219>
- [20] A. Anssari-Benam, A. Bucchi, G. Saccomandi. Modelling the Inflation and Elastic Instabilities of Rubber-Like Spherical and Cylindrical Shells Using a New Generalised Neo-Hookean Strain Energy Function. Journal of Elasticity (2021). <https://doi.org/10.1007/s10659-021-09823-x>
- [21] D. M. Taghizadeh, A. Bagheri, and H. Darijani. On the Hyperelastic Pressurized Thick-Walled Spherical Shells and Cylindrical Tubes Using the Analytical Closed-Form Solutions. International Journal of Applied Mechanics. 07(2015) No. 02, 1550027.
- [22] G. deBotton, R. Bustamante, A. Dorfmann. Axisymmetric bifurcations of thick spherical shells under inflation and compression. International Journal of Solids and Structures, 50 (2), 403-413, 2013. <https://doi.org/10.1016/j.ijsolstr.2012.10.004>
- [23] M.A. Mooney, A Theory of Large Elastic Deformation. Journal of Applied Physics, 11, 582-592, 1940. <https://doi.org/10.1063/1.1712836>
- [24] A. N. Gent, & A. G. Thomas. Forms of the stored (strain) energy function for vulcanized rubber. Journal of Polymer Science 28, 625-637, 1958. <https://doi.org/10.1002/pol.1958.1202811814>
- [25] A. Isihara, N. Hashitsume, & M. Tatibana, Statistical Theory of Rubber - Like Elasticity. IV. (Two - Dimensional Stretching). The Journal of Chemical Physics, 19 (12), 1508-1512, 1951. <http://dx.doi.org/10.1063/1.1748111>
- [26] V. L. Biderman, Calculations of rubber parts (enrusse). RaschetinaProchnost, 40 (1958).